Int. J. Heat Mass Transfer. Vol. 36, No. 7, pp. 1867–1874, 1993
Printed in Great Britain

0017-9310/93 $6.00+0.00

The influence of external heat transfer on flame extinction of dilute sprays

SHUHN-SHYURNG HOU, CHI-CHANG LIU and TA-HUI LIN†
Department of Mechanical Engineering, National Cheng-Kung University, Tainan, Taiwan 701, Republic of China

(*Received* 2 *January* 1992 *and in final form* 12 *August* 1992)

Abstract—The extinction of a dilute spray flame burning in a steady, one-dimensional, low-speed, sufficiently off-stoichiometric, two-phase flow, and experiencing the external heat transfer from the spray to a tube wall upstream is further analyzed. The external heat transfer results in globally external heat loss, excess enthalpy burning and external heat gain, respectively, to the spray system with increasing the wall temperature. However, the droplet gasification provides the overall internal heat loss and heat gain for rich and lean sprays, respectively. Therefore, the burning and extinction of the dilute spray flame can be fully described by the interaction between external and internal heat transfers in two spray models which were identified to be the completely and partially prevaporized burnings. The C-shaped and S-shaped extinction curves are clearly classified and mapped with parameters of the wall temperature, the overall external heat transfer and the initial droplet size. Variations of the extinction curves under the influence of transition from overall external heat loss to heat gain, and the jump between the completely and partially prevaporized burnings on flame extinction, are reported and discussed for both lean and rich sprays.

1. INTRODUCTION

IN THE theory of laminar flame propagation for dilute sprays [1, 2], it was generally concluded that the qualitatively different behavior of lean and rich sprays can be described on the basis of the reduction of the gas-phase fuel concentration through mixture heterogeneity, such that the burning intensities of lean and rich sprays are respectively reduced and enhanced. Lin *et al.* [1] particularly pointed out that for a lean spray, the liquid fuel absorbs heat for upstream prevaporization, produces the secondary gasified fuel for the bulk gas-phase burning, burns through droplet combustion afterwards, and finally results in the internal heat gain. On the other hand, the secondary gasified fuel in a rich spray is equivalent to an inert without any contribution to burning, thereby producing the internal heat loss to the spray system. Therefore, the influence of internal heat gain or heat loss through the droplet gasification process on the flame propagation of dilute sprays has been subsequently studied by Huang *et al.* [3] in non-conserved systems which have constant gas-phase concentrations and various amounts of liquid loading. Results showed that for a rich spray, flame extinction can be identified from an S-shaped curve (a triple-valued function) if the rich spray is thick enough and consists of liquid droplets large enough, while no flame extinction occurs for a lean spray.

In order to compare them [3] with the flame-quenching theory [4] of laminar premixtures by heat loss, shown as a C-shaped curve (a double-valued function), Liu and Lin [5] recently allowed the dilute spray system to experience the external heat loss upstream of the premixed flame, through heat conduction from the spray to a tube wall maintained at the constant inlet temperature ($T_{-\infty}$). Using the same orders of magnitude in spray mass and the external heat loss, they found that there only exist C-shaped extinction curves for both lean and rich sprays. However, the C-shaped curves can be modified by varying the liquid status in sprays, such as the initial droplet sizes ($r'_{-\infty}$) and the amount of liquid fuel loading (γ).

The competition between external and internal heat losses on the flame extinction of dilute sprays had been further emphasized [6] by the enhancement of upstream prevaporization which is achieved by increasing the wall temperature (T_u). In the case of $T_u > T_{-\infty}$, it was noted that the upstream spray experiences the external heat gain and heat loss when T_u is respectively higher and lower than the flow temperature. For the completely prevaporized burning (CPB) spray in which liquid droplets complete evaporation before reaching the bulk premixed flame, the extinction curve was independent of the enhancement of the upstream prevaporization. However, the enhancement of upstream prevaporization, influenced by a higher value of the wall temperature, weakens the partially prevaporized burning (PPB) of both lean and rich sprays.

The extinction characteristics of dilute spray by the enhancement of upstream prevaporization are briefly summarized here by using Figs. 1 and 2 adopted from the previous report [6]. Figures 1 and 2 show the flame flux on extinction ($\dot{m}_E$) as a function of the external

† Author to whom correspondence should be addressed.

NOMENCLATURE

Dimensional quantities

B'	frequency factor
c'_{PG}	specific heat
$\tilde{M}'$	average molar mass
$\dot{m}'_P$	mass flux of a homogeneous premixture
Q'	heat of combustion per unit mass of fuel
$\tilde{R}$	universal gas constant.

Non-dimensional quantities

A	equation (5)
h_{LG}	latent heat of vaporization, h'_{LG}/Q'
K	heat transfer coefficient, $\lambda' K'/c'_{PG}\dot{m}'^2_P$
$\dot{m}$	normalized mass flux
Q_L	external heat transfer parameter
T	temperature, $T'c'_{PG}/Q'$
T_a	activation temperature
x	transformed coordinate
Y	$Y_F = Y'_F$ and $Y_O = Y'_O/\sigma$
Z	ρ'_G/ρ'.

Greek symbols

γ	$(1-Z_{-\infty})/\varepsilon$
ε	small expansion parameter, T_∞/T_a
ξ	equation (6)
σ	stoichiometric ratio
ϕ	equivalence ratio.

Superscripts and subscripts

*	critical conditions
′	dimensional quantities
b	boiling state
e	state at which droplet is completely gasified
E	state at extinction
f	flame front
F, O	fuel and oxygen
G, L	gas and liquid phases
v	state at which vaporization initiates
$-\infty, \infty$	initial and final states.

heat loss (Q_L) for various values of $r'_{-\infty}$ and T_u for a lean ($\phi_G = 0.8$, $\gamma = 0.02$) and a rich ($\phi_G = 2.0$, $\gamma = 0.3$) spray, respectively. Curves denoted by $\gamma = 0$ and $r'_{-\infty} \leqslant r'_c$ represent the extinction curves of homogeneous premixtures and a CPB spray, respectively. It is clearly shown that there is a minimum wall temperature $T_u = 510.5$ and 477.2 K in Figs. 1 and 2, respectively, to allow a jump from the CPB to PPB along the $\dot{m}_E$ line. If T_u is larger than the minimum wall temperature, a critical value of the initial droplet radius ($r'^*_{-\infty}$), will then be determined to show that the extinction curve of a spray having $r'_{-\infty} < r'^*_{-\infty}$ is composed of an upper branch representing the PPB and a lower branch showing the CPB, e.g. $r'^*_{-\infty} = 49.4$ μm at $T_u = 650$ K in Fig. 1 and $r'^*_{-\infty} = 38.7$ μm at $T_u = 650$ K in Fig. 2. The flame extinction is now controlled by the CPB which is originally identified to be unstable in the absence of the enhancement of upstream prevaporization. On the other hand, for a spray having $r'_{-\infty} \geqslant r'^*_{-\infty}$, the flame extinction is totally controlled by the PPB, and the S-shaped curve is reproduced to be inserted into the C-shaped curve.

From the results described above, one may expect that flame extinction of a spray having both $r'_{-\infty}$ and T_u large enough is strongly influenced by the internal heat transfer associated with the droplet gasification process. This phenomenon is similar to that of flame extinction of dilute sprays without external heat transfer [3]. However, in this preliminary investigation [6], the importance of external heat transfer was limited by the calculated value of T_u, up to 650 K. In the range of selected T_u, the spray experiences simultaneously the external heat gain and heat loss upstream, but has a net amount of external heat loss

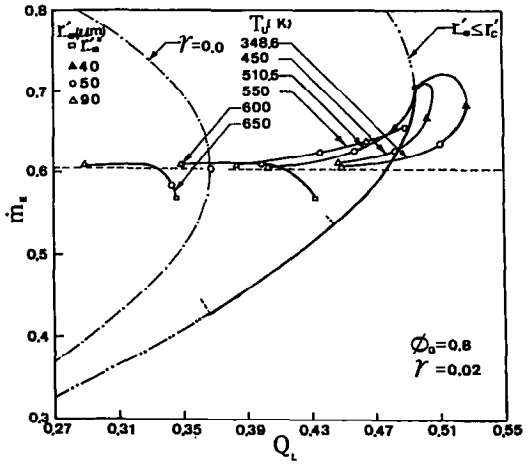

FIG. 1. The flame flux at extinction $\dot{m}_E$ as functions of the external heat loss Q_L, the initial droplet radius $r'_{-\infty}$ and the wall temperature T_u, for a lean spray.

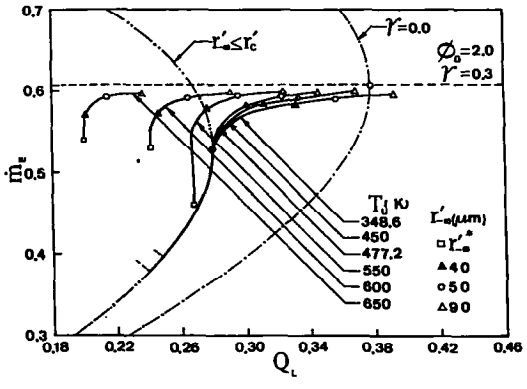

FIG. 2. The flame flux at extinction $\dot{m}_E$ as functions of the external heat loss Q_L, the initial droplet radius $r'_{-\infty}$ and the wall temperature T_u, for a rich spray.

shown by a positive value of Q_L. The parameter of external heat transfer Q_L is determined by the upstream integration of the energy equation and energy balance between far upstream and far downstream, and reflects the magnitude of overall external heat transfer. Therefore, we note that by varying T_u, the spray system may globally have external heat loss, no external heat transfer and external heat gain for the cases of $Q_L > 0$, $Q_L = 0$ and $Q_L < 0$, respectively. The case of $Q_L = 0$ is closely related to the excess enthalpy burning proposed by Weinberg [7]. Taking a general view of the possibility of external heat transfer, one realizes that the interaction between external and internal heat transfer plays an important role in fully describing the extinction and burning characteristics of dilute sprays.

In this report, we extend the preliminary results [5, 6] to cover the whole range of external heat transfer. The transition from overall external heat loss to overall external heat gain and the jump from the completely prevaporized burning to the partially prevaporized burning on flame extinction will be investigated with parameters of the wall temperature and the initial droplet radius. The mathematical technique used is the matched asymptotic analysis in the limit of large activation energy. We shall also restrict our analysis to dilute spray with the amount of liquid loading being of $O(\varepsilon)$ of the total spray mass, and to the external heat transfer being of $O(\varepsilon)$ in the upstream region of the bulk premixed flame. The small parameter of expansion ε is the ratio of thermal energy to activation energy in the combustion process.

2. THEORETICAL MODEL

We adopt a one-dimensional coordinate system in which the premixed flame sits at the origin ($x = 0$), the two-phase combustible mixture approaches from $x = -\infty$ and equilibrium reaction products move away toward $x = +\infty$, as shown in Fig. 3. By defining a critical droplet size (r'_c) for droplets to achieve complete evaporation at the premixed flame front, we have completely prevaporized burning (CPB) and partially prevaporized burning (PPB) for sprays of $r'_{-\infty} \leqslant r'_c$ and $r'_{-\infty} > r'_c$, respectively. We assume that droplets will start to vaporize, at $x = x_v$, only when the gas temperature has reached the boiling point of the liquid. Droplets then ignite upon crossing the flame, and will extinguish at $x = x_e$ upon complete depletion of the oxygen in the gas mixture. However, in the case of rich sprays, only droplet vaporization is possible and x_e indicates the complete evaporation of droplets. We further assume that the external heat transfer is proportional to $(T - T_u)$, and occurs in the upstream region of x_v to 0. Finally, we assume that the fuel and oxidizer reaction for the bulk premixed flame is one-step overall, that the fuel droplets burn in the flame-sheet limit, and that constant property simplification applies.

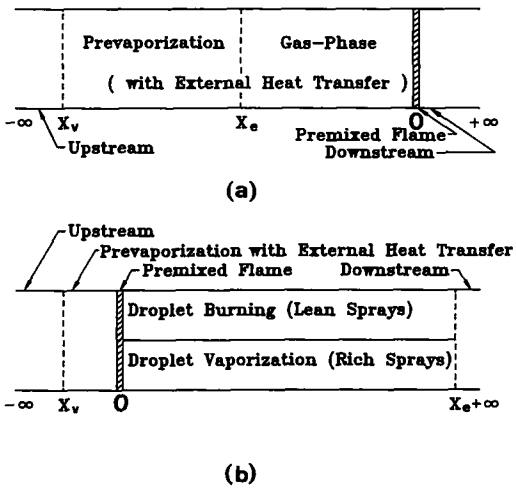

FIG. 3. Schematic diagram of (a) completely prevaporized, and (b) partially prevaporized burning sprays.

The conservation equations for heat and mass are given in Liu and Lin [5]. We designated the extent of gas-phase heterogeneity by the parameter $Z = \rho'_G/\rho'$ such that $Z = 1$ represents the completely vaporized state. Then, the non-dimensional equations for gas-phase continuity, and conservation of fuel, oxidizer and energy are, respectively, given by

$$Z\dot{m}\frac{dZ}{dx} = \frac{A}{T}(1-Z_{-\infty})^{2/3}(1-Z)^{1/3}F(T, Y_O) \quad (1)$$

$$\frac{d}{dx}(Z\dot{m}Y_F - \frac{d}{dx}Y_F) = \dot{\xi} + f_F\dot{m}\frac{dZ}{dx} \quad (2)$$

$$\frac{d}{dx}\left(Z\dot{m}Y_O - \frac{d}{dx}Y_O\right) = \dot{\xi} + f_O\dot{m}\frac{dZ}{dx} \quad (3)$$

$$\frac{d}{dx}\left(Z\dot{m}T - \frac{d}{dx}T\right) = -\dot{\xi} + f_T\dot{m}\frac{dZ}{dx} - \varepsilon K(T-T_u)H(0) \quad (4)$$

where

$$A = 3\left(\frac{\lambda'}{r'_{-\infty}\dot{m}'_P}\right)^2\left(\frac{P'\bar{M}'}{\bar{R}c'_{PG}Q'\rho'_L}\right) \quad (5)$$

$$\dot{\xi} = -\left(\frac{B'\sigma}{\bar{M}'_O}\right)\left(\frac{P'\bar{M}'}{\bar{R}}\right)^2\left(\frac{\lambda'}{c'_{PG}\dot{m}'^2_P}\right)Y_O Y_F \exp\left(-\frac{T_a}{T}\right) \quad (6)$$

and the function

$$H(0) = \begin{cases} 1 & \text{for } x_v \leqslant x \leqslant 0 \\ 0 & \text{for } x > 0 \end{cases} \quad (7)$$

while x is the non-dimensional distance expressed in units of the preheat zone thickness. In equations (1)–(4), the function $F(T, Y_O)$ and the constant parameters f_F, f_O and f_T are, respectively, $\ln[1+(T-T_b)/h_{LG}]$, 1, 0, $-h_{LG}$ for the vaporizing droplet and $\ln[1+(T-T_b-Y_O)/h_{LG}]$, 0, -1 and $(1-h_{LG})$ for the burning droplet. K and $\dot{m}$ denote the

heat transfer coefficient for the external heat transfer, and the flame propagation flux normalized by the premixed value, $\dot{m}'_p$.

Performing the inner and outer expansions, and following the detailed matching procedure of ref. [5] to match the inner and outer solutions, we have final results as follows:

$$\dot{m}^2 = \exp[T_1^+(0)] \tag{8}$$

indicating that the flame propagation flux is exponentially affected by the first-order temperature downstream near the flame. The amount of $T_1^+(0)$ can be expressed by equation (19) in ref. [5] with an additional term such as

$$\left(\frac{1-e^{-\dot{m}x_c}}{e^{-\dot{m}x_c}-e^{-\dot{m}x_v}}\right) \times\left[\frac{K(T_{-\infty}-T_u)}{\dot{m}^2 T_\infty}(1-\dot{m}x_v e^{-\dot{m}x_v}-e^{-\dot{m}x_v})\right]. \tag{9}$$

Setting $Z = 1$ to approach the condition of a homogeneous premixture, we obtain

$$\dot{m}^2 \ln(\dot{m}^2) = -Q_L \tag{10}$$

where the parameter

$$Q_L = K\left[\frac{(T_\infty - T_b)}{T_\infty} - \frac{(T_{-\infty}-T_u)}{T_\infty}\ln\left(\frac{T_b - T_{-\infty}}{T_\infty - T_{-\infty}}\right)\right] \tag{11}$$

shows the net influence of external heat transfer. As $T_u = T_{-\infty}$, equation (9) and the second term of equation (11) vanish to result in $Q_L > 0$ showing that the spray endures not only locally but also globally external heat loss discussed in ref. [5]. By increasing T_u, the upstream spray starts to have both external heat loss and heat gain simultaneously, and the magnitude of Q_L begins to decrease. At the condition of $Q_L = 0$, heat is transferred through the tube wall from the high-temperature region ahead of the flame to the low-temperature region, and the net heat transfer to the spray system is zero. This is the so-called excess enthalpy burning [7]. An overall external heat gain ($Q_L < 0$) can be achieved as the wall temperature is large enough.

Q_L and T_u corresponding to the external heat transfer, and $r'_{-\infty}$ and γ associated with the internal heat transfer are selected as parameters in the calculation. Sample calculations for *n*-octane (C_8H_{18}) burning in air are now considered in a non-conserved manner which maintains the initial gas-phase composition but varies the liquid fuel loading systematically. The relevant physical properties are referred to the earlier studies [1, 3]. Results for lean and rich sprays are separately discussed in the following sections.

3. LEAN SPRAYS

Figure 4 shows the map of possible extinction curves for a lean spray of $\phi_G = 0.8$ and $\gamma = 0.02$. The

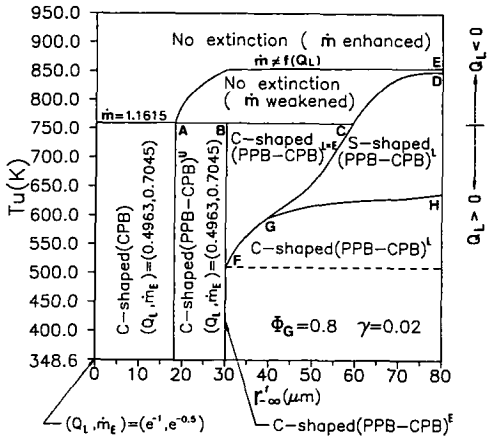

FIG. 4. The map of possible burning and extinction curves for a lean spray.

corresponding extinction curves for $T_u = 700$, 759.72 and 800 K are also presented in Figs. 5–7, respectively. The point of $(T_u, r'_{-\infty}) = (348.6\text{ K}, 0\ \mu\text{m})$ in Fig. 4 corresponds to a homogeneous premixture enduring the external heat loss under $T_u = T_{-\infty}$. Therefore, the flame flux at extinction and the associated heat loss are, respectively, equal to $e^{-0.5}$ and e^{-1} which were identified by the flame-quenching theory [4] before. In the region of $T_u < 759.72$ K and $r'_{-\infty} < 18.32\ \mu$m, there exists only a C-shaped extinction curve under CPB conditions as shown by a dot-dash line in Fig. 5. The $\dot{m}_E$ and the corresponding Q_L are constants in this region and larger than those of the homogeneous premixture. This is caused by the additional heat gain through burning the secondary gasified fuel from the droplet gasification process for a lean spray. As $T_u < 759.72$ K and $18.32\ \mu\text{m} < r'_{-\infty} < 30.2\ \mu$m in Fig. 4, C-shaped extinction curves are shown which are composed of a line of PPB spray and a curve of CPB spray with the junction on the upper branch of CPB sprays. With increasing the $r'_{-\infty}$, the junction shifts toward the extinction point of the CPB spray along the dot-dash line, as shown in Fig. 5. However, the extinction conditions in such circumstances remain constant, $(Q_L, \dot{m}_E) = (0.4963, 0.7045)$. In Fig. 4, the superscripts denoted by U, E and L represent the

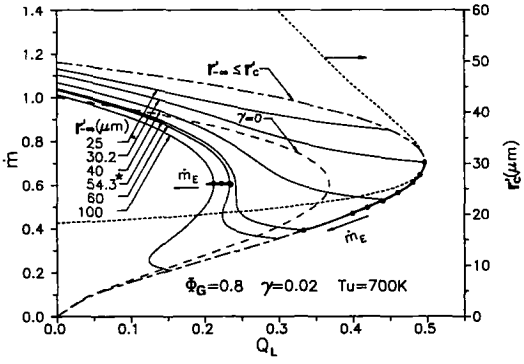

FIG. 5. The flame flux $\dot{m}$ as functions of the external heat loss Q_L and the initial droplet radius $r'_{-\infty}$ for a lean spray at $T_u = 700$ K.

junctions of PPB–CPB curves occurring at the upper branch, the extinction condition and the lower branch of the CPB extinction curve, respectively.

The area underneath the FGH line in Fig. 4 shows that the PPB–CPB extinction curves have the junctions on the lower branch of the CPB curve, and their flame extinctions are identified under the PPB condition, as described before [6]. It is further found that as $T_u < 510.5$ K (area underneath the dashed line in Fig. 4), the flame flux at extinction ($\dot{m}_E$) first increases, then decreases, and finally approaches $e^{-0.5}$ with the increase of the droplet radius [5]. However, at the condition of $T_u = 510.5$ K, the extinction curves of PPB sprays are shifted inside the envelope of the CPB extinction curve, and the corresponding $\dot{m}_E$ decrease monotonically with an increase in $r'_{-\infty}$, as shown in Fig. 1.

In the region of BCGF in Fig. 4, the extinction curve consists of an upper branch corresponding to the PPB, a lower branch associated with the CPB, and a junction which belongs to the unstable branch of the CPB and shows flame extinction. This extinction curve can be shown by the curve of $r'_{-\infty} = 40$ μm at $T_u = 700$ K in Fig. 5. For the case of $T_u = 550$ K, we had found [6] that by increasing $r'_{-\infty}$ beyond 33 μm (crossing line FG in Fig. 4), the flame extinction occurs at the condition of PPB instead of that of unstable CPB. This phenomenon was clearly presented in the Introduction. From Fig. 4, it is noted that there exists a minimum wall temperature (510.5 K) to allow a jump from the CPB to the PPB along the $\dot{m}_E$ line (Fig. 1) by passing through line FG in which $r'_{-\infty} = r'^*_{-\infty}$, identified before.

In considering a higher value of T_u, e.g. $T_u = 700$ K in Figs. 4 and 5, we understand that by increasing the initial droplet radius, the upstream prevaporization can be enhanced to intensify the influence of the internal heat transfer on the spray extinction. Therefore, an S-shaped extinction curve is reproduced on the basis of the spray having $r'_{-\infty}$ and T_u large enough, as restricted in the region of GCDH in Fig. 4. In the case of $T_u = 700$ K, the $\dot{m}_E$ line still jumps from CPB to PPB at $r'^*_{-\infty} = 54.3$ μm (on line GC in Fig. 4).

According to the energy balance upstream of the premixed flame, the overall external heat transfer is zero as $T_u = 759.72$ K, which is uniquely determined for a spray of $\phi_G = 0.8$ and $\gamma = 0.02$, and independent of the heat transfer coefficient K and the initial droplet radius. The extinction curves in response of K and $r'_{-\infty}$ for $Q_L = 0$ are presented in Fig. 6. It is clearly shown that no flame extinction occurs for the homogeneous premixture and the CPB spray, and the flame flux of the CPB spray is higher than that of the homogeneous premixture because of the additional internal heat gain for a lean spray. We further find that as $r'_{-\infty} < 59.4$ μm, the $\dot{m}$ value is monotonically decreased by increasing the heat transfer coefficient, resulting in no flame extinction. Moreover, the S-shaped extinction curve governed by the PPB spray is

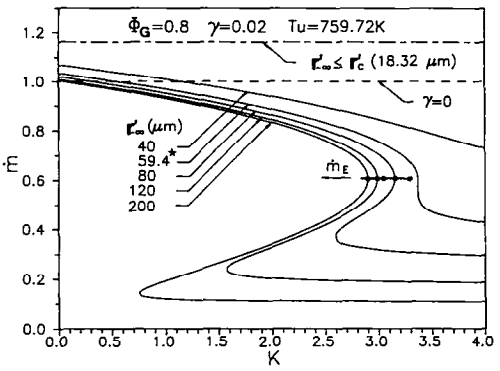

FIG. 6. The flame flux $\dot{m}$ as functions of the external heat transfer coefficient K and the initial droplet radius $r'_{-\infty}$ for a lean spray at $T_u = 759.72$ K.

obtained for a droplet size larger than 59.4 μm, as shown in Fig. 6.

By further increasing the wall temperature, e.g. $T_u = 800$ K, the external heat transfer gives an external heat gain denoted by $Q_L < 0$ in Fig. 4. Therefore, the burning intensities of the homogeneous premixture and the CPB spray are strengthened with the increase in magnitude of external heat gain as shown in Fig. 7. Figure 7 shows that there exists an initial droplet radius to allow for the flame flux of a PPB spray being independent of the Q_L, i.e. 20.79 μm (on line AE in Fig. 4). As $r'_{-\infty} < 20.79$ μm and $r'_{-\infty} > 20.79$ μm, the $\dot{m}$ are, respectively, enhanced and weakened in response to increasing the external heat gain. Flame extinction can be found as the spray has a droplet radius larger than 63.5 μm at $T_u = 800$ K. It is interesting to note that for a very large value of $r'_{-\infty}$ (200 μm in Fig. 7), the $\dot{m}_E$ and the magnitude of Q_L are closely equal to $e^{-0.5}$ and e^{-1}, respectively. Finally, as we increase T_u approximately above 854 K, the flame flux of the homogeneous premixture, CPB spray and PPB spray are enhanced by the internal heat gain, resulting in no flame extinction.

The variation of the extinction curve for a spray of $\phi_G = 0.8$ and $\gamma = 0.02$, having $r'_{-\infty} = 40$ and 80 μm, with different values of T_u are shown in Figs. 8 and 9, respectively. Figure 8 shows that as $T_u < 598$ K, the

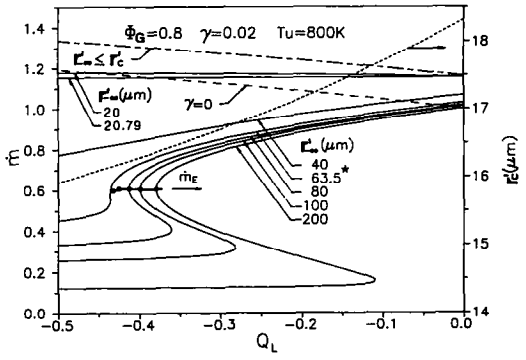

FIG. 7. The flame flux $\dot{m}$ as functions of the external heat gain Q_L and the initial droplet radius $r'_{-\infty}$ for a lean spray at $T_u = 800$ K.

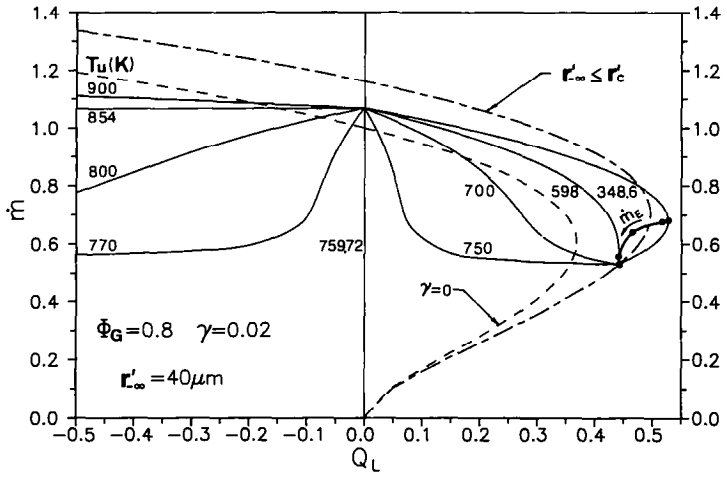

FIG. 8. The flame flux $\dot{m}$ as functions of T_u and Q_L for a lean spray having $r'_{-\infty} = 40$ μm.

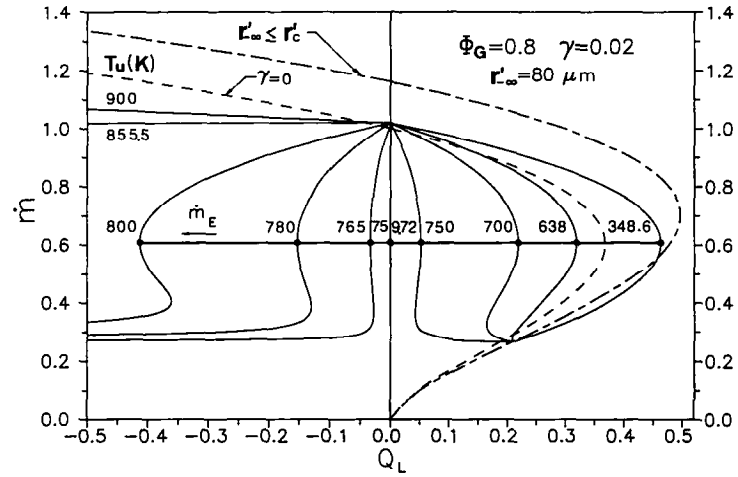

FIG. 9. The flame flux $\dot{m}$ as functions of T_u and Q_L for a lean spray having $r'_{-\infty} = 80$ μm.

flame extinction is controlled by the PPB, and the corresponding $\dot{m}_E$ decreases to the condition of the CPB spray ($r'_c = 40$ μm) by increasing T_u. The condition of $(T_u, r'_{-\infty})$ = (598 K, 40 μm) is located on the line FG in Fig. 4. If we increase T_u further, the flame flux of PPB spray (the upper branch of the extinction curve) is weakened, however, the lower branch of the curve and the condition of flame extinction remain the same. In the circumstance of $T_u = 750$ K, it reflects that the $\dot{m}$ of steady burning has rapid response to the small Q_L, but is insensitive to the large Q_L before flame extinction. No flame extinction occurs for $T_u > 759.72$ K, shown in Figs. 4 and 8. For the spray having largest droplet radius, $r'_{-\infty} = 80$ μm in Fig. 9, the flame extinction is achieved under the PPB condition in the whole range of T_u variation. It is important to note that the $\dot{m}_E$ is independent of T_u and Q_L, and closely equal to $e^{-0.5}$ in Fig. 9.

4. RICH SPRAYS

For a rich spray of $\phi_G = 2.0$ and $\gamma = 0.3$, the possible extinction curves are classified on the map in Fig. 10, and illustrated in Figs. 11–13 for $T_u = 700$, 736.23 and 800 K, respectively. The map of the rich spray (Fig. 10) is similar to that of the lean spray (Fig. 4), except that the $\dot{m}_E$ and the corresponding Q_L for the

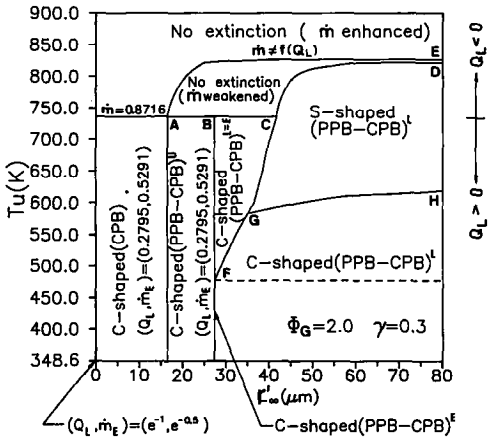

FIG. 10. The map of possible burning and extinction curves for a rich spray.

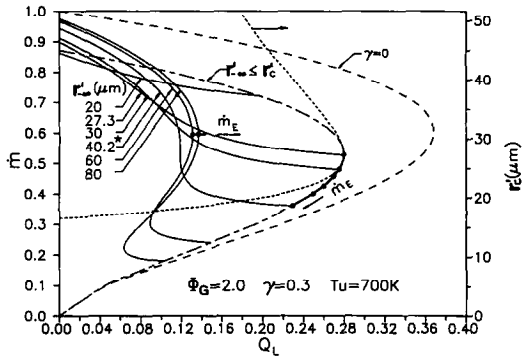

FIG. 11. The flame flux $\dot{m}$ as functions of the external heat loss Q_L and the initial droplet radius $r'_{-\infty}$ for a rich spray at T_u = 700 K.

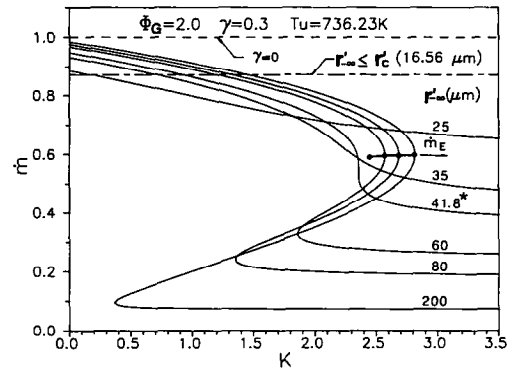

FIG. 12. The flame flux $\dot{m}$ as functions of the external heat transfer coefficient K and the initial droplet radius $r'_{-\infty}$ for a rich spray at T_u = 736.23 K.

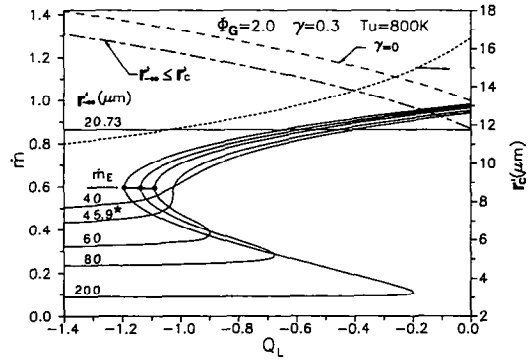

FIG. 13. The flame flux $\dot{m}$ as functions of the external heat gain Q_L and the initial droplet radius r'_{∞} for a rich spray at T_u = 800 K.

CPB spray are respectively smaller than $e^{-0.5}$ and e^{-1} because only the internal heat loss occurs in the droplet gasification process. Under the specified condition of the rich spray, the T_u for $Q_L = 0$ and the minimum T_u allowing a jump from the CPB to the PPB along the $\dot{m}_E$ line, are determined to be 736.23 and 477.2 K, respectively.

Figure 11 shows that as $r'_{-\infty} < 27.3$ μm, the flame extinction is identified under the extinction point of the CPB curve. By continuously increasing $r'_{-\infty}$ larger than 27.3 μm, the extinction condition varies along the lower branch of the CPB curve, and jumps onto the S-shaped extinction curve of the PPB spray as $r'_{-\infty} = 40.2$ μm (on line GC of Fig. 10). For the case of excess enthalpy burning ($Q_L = 0$ at $T_u = 736.23$ K), it is found that no flame extinction occurs for the CPB spray and the homogeneous premixture, and flame extinction can be achieved for the PPB spray having $r'_{-\infty}$ larger than 41.8 μm, shown in Fig. 12. As T_u = 800 K, Fig. 13 shows that the $\dot{m}$ of the homogeneous premixture, the CPB spray and the PPB spray having $r'_{-\infty} < 20.73$ μm are increased monotonically by increasing the strength of external heat gain. However, the flame extinction occurs as $r'_{-\infty} > 45.9$ μm (on line CD of Fig. 10).

Finally, a typical variation of the $\dot{m}$ curve in response to T_u for a rich spray of $\phi_G = 2.0$, $\gamma = 0.3$ and $r'_{-\infty} = 40$ μm can be explored by using Figs. 2 and 10–13. As $T_u = T_{-\infty} = 348.6$ K [5, 6], the $\dot{m}$ curve is located between the envelopes of the homogeneous premixture and the CPB spray. The $\dot{m}_E$ and Q_L at extinction are decreased with increasing the T_u. This shows that a rich spray flame experiencing larger values of T_u will be extinguished earlier due to the enhanced upstream prevaporization. A jump from the PPB to the CPB at extinction occurs approximately at T_u = 699 K in Fig. 10. As $T_u > 736.23$ K, the overall external heat gain ($Q_L < 0$) prevents the spray flame from extinction.

5. CONCLUSIONS

We have further investigated extinction of the dilute spray flame which is burning in a steady, one-dimensional, low-speed, sufficiently off-stoichiometric, two-phase flow, and experiencing the external heat transfer from the spray to a tube wall upstream. A completely prevaporized burning model and a partially prevaporized burning model were identified on the basis of liquid droplet size for completing evaporation before the bulk flame. By varying the wall temperature, the spray system may globally experience external heat loss, excess enthalpy burning and external heat gain, respectively. On the other hand, the lean and rich sprays have overall internal heat gain and heat loss, respectively, through the droplet gasification process.

The burning and extinction of the dilute spray flame were fully described by the interaction between external and internal heat transfers in different spray burning models. The C-shaped and S-shaped extinction curves were classified and mapped in response to the wall temperature and the initial droplet size. As the wall temperature was higher than a certain minimum, it was found that the flame extinction may be achieved on the condition of the completely prevaporized burning which is originally identified to be unstable in the absence of the enhancement of upstream prevaporization; and that the line of flame flux at extinction has a jump between the completely and partially

prevaporized burnings by varying the initial droplet size.

In view of this theoretical result, we realize that the understanding on flame extinction of dilute sprays should be further justified by the experiment, and further explored in considering a more realistic model with advanced numerical and theoretical techniques. From the open literature, it would be useful to suggest that the experimental set-up for combustion of liquid fuel spray in stagnation-point flow [8] and the modeling of counterflow spray combustion [9] could be used in advancing our recent results.

Acknowledgement—This work was supported by the National Science Council, Taiwan, R.O.C. under contract NSC79-0401-E006-20.

REFERENCES

1. T. H. Lin, C. K. Law and S. H. Chung, Theory of laminar flame propagation in off-stoichiometric dilute sprays, *Int. J. Heat Mass Transfer* **31,** 1023–1034 (1988).
2. T. H. Lin and Y. Y. Sheu, Theory of laminar flame propagation in near-stoichiometric dilute sprays, *Combust. Flame* **84,** 333–342 (1991).
3. C. L. Huang, C. P. Chiu and T. H. Lin, The influence of liquid fuel on the flame propagation of dilute sprays in non-conserved systems, *J. CSME* **10,** 333–343 (1989).
4. J. D. Buckmaster and G. S. S. Ludford, *Theory of Laminar Flames*, p. 38. Cambridge University Press, Cambridge (1982).
5. C. C. Liu and T. H. Lin, The interaction between external and internal heat losses on the flame extinction of dilute sprays, *Combust. Flame* **85,** 468–478 (1991).
6. C. C. Liu and T. H. Lin, The influence of upstream prevaporization on flame extinction of one-dimensional dilute sprays. In *Aerothermodynamics in Combustors* (Edited by Richard S. L. Lee and J. H. Whitelaw), pp. 199–211. Springer, Berlin (1992).
7. F. J. Weinberg, Combustion temperatures: the future? *Nature* **233,** 239–241 (1971).
8. Z. H. Chen, T. H. Lin and S. H. Sohrab, Combustion of liquid fuel sprays in stagnation-point flow, *Combust. Sci. Tech.* **60,** 63–77 (1988).
9. G. Continillo and W. A. Sirignano, Counterflow spray combustion modeling, *Combust. Flame* **81,** 325–340 (1990).